



The X-ray emission of magnetic cataclysmic variables in the XMM-Newton era

M. Mouchet^{1,2}, J.M. Bonnet-Bidaud³, and D. de Martino⁴

¹ Laboratoire Astroparticule et Cosmologie, Université Paris Diderot – F-75013 Paris, France, e-mail: martine.mouchet@apc.univ-paris-diderot.fr

² Laboratoire LUTH, Observatoire de Paris, CNRS, Université Paris-Diderot, F-92190 Meudon, France

³ CEA Saclay, DSM/Irfu/Service d'Astrophysique, F-91191 Gif-sur-Yvette, France

⁴ INAF Capodimonte Observatory, Salita Moiariello 16, I-80131 Napoli, Italy

Abstract. We review the X-ray spectral properties of magnetic cataclysmic binaries derived from observations obtained during the last decade with the large X-ray observatories XMM-Newton, Chandra and Suzaku. We focus on the signatures of the different accretion modes which are predicted according to the values of the main physical parameters (magnetic field, local accretion rate and white dwarf mass). The observed large diversity of spectral behaviors indicates a wide range of parameter values in both intermediate polars and polars, in line with a possible evolutionary link between both classes.

Key words. Stars: novae, cataclysmic variables – Stars: white dwarfs – Stars: magnetic field – X-rays: binaries – accretion, accretion disks

1. Introduction

In magnetic cataclysmic binaries, the magnetic field of the white dwarf is strong enough to channel the accreting matter along the field lines from the magnetosphere. Material thus falls down close to the polar caps, along an accretion column or curtain. Two main categories are distinguished: the synchronous Polars (AM-Her type) and the non-synchronized Intermediate Polars (IPs) ($P_{spin} < P_{orb}$).

More than one hundred polars are presently known (Ritter & Kolb (2003) catalog, version June 2011), having orbital/spin periods ranging from 77 min. to 14 h with more than a half having a period below the evolutionary gap (be-

low 2h). Their magnetic fields have been determined by different methods (cyclotron lines, Zeeman components, optical polarimetry) and their values range between 7 and 230 MG (Wickramasinghe & Ferrario 2000, Gänsicke et al. 2004). Polars often exhibit alternate high and low states, associated with variations of the accretion rates (10^{10} to $10^{-13} M_{\odot} \text{ yr}^{-1}$). For seven of them, the white dwarf rotation differs slightly from the orbital one by a few percent. IPs are less numerous (36 secure and 20 probable in Mukai (2011) catalog, version Jan. 2011). Their orbital periods range from 80 min. to 48 h, with only 5 objects below the gap, and with spin-to-orbital period ratios ranging from 9×10^{-4} to 0.68. For eight sources, polarized optical flux has been detected with estimates of the magnetic field between 8 to 15 MG, ex-

cept for V405 Aur (30 MG) (Katajainen et al. 2010). The accretion occurs directly from the disc (disc-fed), possibly with a stream overflow and, for at least one source (V2400 Oph), with no disc (Hellier 2007). The accretion geometry strongly depends on the combination of the accretion rate and B values (Norton et al. 2008). As already extensively debated, whether or not IPs are progenitors of polars, with similar magnetic field values, is still an open question.

2. The accretion models

2.1. The standard shock model

The basic picture of the accretion onto a magnetic white dwarf consists in a field aligned flow directed to the magnetic poles which is shocked before reaching the WD surface, with most of the gravitational energy released in the post-shock region (PSR). The resulting shock temperature is given by $T_s = 3GMm_h/8kR$, of the order of 10 to 50 keV (M and R being the WD mass and radius). The corresponding X-ray luminosity $L_X = GMM_{dot}/R$ is of the order of $10^{31} - 10^{33} \text{ erg s}^{-1}$ (M_{dot} being the accretion rate). Below the shock, bremsstrahlung and cyclotron radiation are the two main competitive cooling processes. Hard X-rays ($E > 2 \text{ keV}$) are radiated from the post-shock plasma as well as optical/IR cyclotron. Half of the accreting luminosity illuminates the polar caps and is reprocessed as soft X-ray blackbody emission ($E < 2 \text{ keV}$) with a temperature $T_{bb} = (L_{acc}/f 8\pi R^2 \sigma)^{1/4}$, of the order of 10 to 50 eV (f being the irradiated fractional area of the stellar surface).

An exhaustive review of the hydrodynamic steady and non-stationary models of the post-shock region emission has been presented by Wu (2000). Since then, further developments have been proposed. They include, for instance, the 2-temperature models, required for strong magnetic fields, low accretion rates and high WD masses (Fischer & Beuermann 2001, Saxton et al. 2005, Imamura et al. 2008), the effect of mass leakage and heating at the WD surface (Wu et al. 2001), the inclusion of the dipole field geometry (Canalle et al. 2005, Saxton et al. 2007), or the generalization of

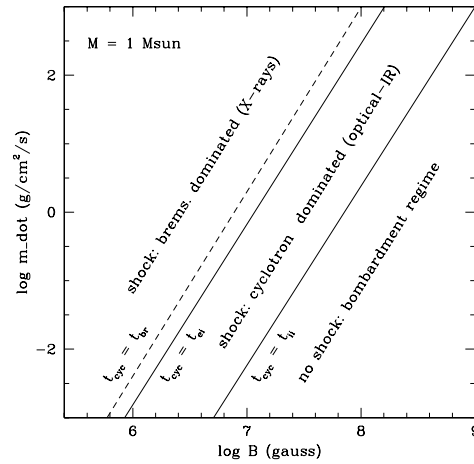


Fig. 1. Regions in the specific accretion rate m_{dot} -B plane of the three accretion regimes (adapted from Lamb & Master 1979).

the analytical solutions (Lamming 2004, Falize et al. 2009) (see also C. Michaut in these proceedings). These studies provide the temperature and density profiles of the post-shock region in the accretion column which in turn allow us to predict the X-ray spectra, via the use of optically thin plasma codes.

2.2. Three main accretion regimes

As originally discussed by King & Lasota (1979) and Lamb & Master (1979), the presence of a stand-off shock strongly depends on the specific local accretion rate m_{dot} and the magnetic field value B. Three main regimes can be distinguished (see Fig.1): a) a *standard shock* is formed above the WD surface for high m_{dot} and low B, b) a *blobby accretion* is expected for very high m_{dot} (Kuijpers et al. 1982, Frank et al. 1988) for which shocks are buried below the WD photosphere, leading to a strong soft X-ray blackbody component and c) a *bombardment regime* is associated with very low m_{dot} and high B (Kuijpers et al. 1982, Woelk & Beuermann 1996 and ref. herein, Fischer and Beuermann 2001). In this last case, Coulomb ion-ion interaction time been longer than the cooling time, this prevents the formation of a

shock. A low temperature X-ray emission is expected for this regime.

X-ray continuum and lines provide powerful diagnostics to probe the temperature and density structures of the accretion column which can be confronted to the predictions of the different regimes. Below we present examples of these three regimes which are encountered in magnetic CVs. Their properties are derived from detailed X-ray observations of IPs and polars, which are now accessible thanks to the new generation of X-ray satellites (XMM-Newton, Chandra and Suzaku) available during the last decade.

3. The accretion modes in intermediate polars

Considering first the intermediate polars, among 36 secure IPs identified at present time, 30 were observed with XMM-Newton, 10 with Chandra and 22 with Suzaku. Eleven of them have been confirmed as IPs using XMM-Newton data which revealed their spin period (see de Martino et al. 2008, Anzolin et al. 2008, Bonnet-Bidaud et al. 2009, Anzolin et al. 2009, de Martino et al. 2009, for the most recent identifications). Numerous IPs are hard X-ray ($E > 20$ keV) sources; 18 were detected with INTEGRAL (Scaringi et al. 2010) and 22 with Swift/BAT (Brunschweiler et al. 2009). Notably the Galactic ridge spectrum is similar to the hard X-ray spectra of IPs (Revnitsev et al. 2009), indicating that they are strong potential contributors to the diffuse galactic hard X-ray emission. The study of their X-ray spectra has thus benefited from their detection at higher energies.

3.1. Hard-X-ray emission and stand-off shocks

For most IPs the cooling below the shock is expected to be dominated by bremsstrahlung radiation. The exact solution of a stationary post-shock region in 1D plane-parallel geometry has been derived by Revnitsev et al. (2004) and found to be very similar to the analytical solution for a constant pressure medium. The temperature and density profiles

depend only slightly from the specific accretion rate and thus, the resulting X-ray spectral shape leads to a direct evaluation of the WD mass (Suleimanov et al. 2005, Yuasa et al. 2010). A possible contribution of Compton up-scattering in the post-shock region has also been evaluated by Suleimanov et al. (2008) but its effect is only significant for high WD masses. The most recent mass determinations using Suzaku data of 17 IPs (Yuasa et al. 2010, see also these proceedings) have been obtained by coupling the PSR structure computed by Suleimanov et al. (2005) with the APEC plasma code (Smith et al. 2001). The derived average mass is $0.88 \pm 0.25 M_{\odot}$, slightly higher than previous estimates (Suleimanov et al. 2005, Brunschweiler et al. 2009).

3.2. Soft X-ray IPs

As mentioned above, the standard shock model predicts a reprocessed component arising from the illumination of the WD surface by the hard X-ray component. Contrary to polars, the first discovered IPs did not show such a component; this was interpreted as due to either a strong absorption in the accretion curtain or to a lower temperature EUV emission associated to a larger irradiated zone. The number of IPs detected in soft X-rays ($E < 1$ keV) has increased from 4 objects seen with ROSAT up to 13 observed with XMM-Newton (about 40%) (Evans & Hellier 2007, Anzolin et al. 2008). When the soft-X-ray component is fitted with a blackbody spectrum (see an example in Fig. 2), the resulting temperatures (typically 50-120 eV) are higher than typically found in polars (20-60 eV) with a lower soft/hard flux ratio (Fig. 3). Yet for polars the accreting surfaces are expected to be smaller than for IPs, implying a higher temperature for a given accretion rate. The higher temperatures found in IPs would indicate higher accretion rates, in line with higher luminosities. The hard X-ray IP emitters being expected to have an undetected reprocessed component shifted in the EUV, the absence of IPs with temperatures similar to those of polars is striking. Such a dichotomy can be related to the magnetic field. Indeed the fact that seven over eight IPs with

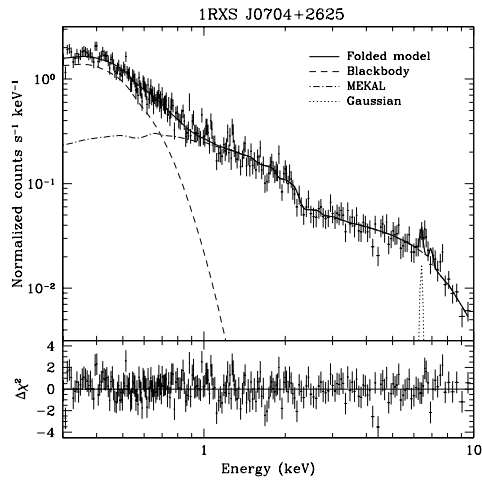


Fig. 2. XMM-Newton EPIC spectrum of the IP 1RXS J070407.9+262501 fitted with a blackbody soft component (dotted line, $T_s=84$ eV) and an optically thin plasma component (dashed-dotted line, $T_h=44$ keV). A gaussian component is added to fit the fluorescence Fe K_α line (from Anzolin et al. 2008).

detectable circular polarisation require a soft X-ray component to be fitted, as for polars, is in favor of the evolutionary link from IPs to polars of similar B values, at least for this subclass of soft IPs. Searches for polarized flux in all soft IPs are strongly needed.

3.3. Additional features of the X-ray spectra

X-ray spectra of IPs are generally well described in the context of the stand-off shock model predicting both hard X-ray and soft X-ray reprocessed emission. However some sources show more complex spectra, exhibiting signatures of partial cold and/or warm absorbers, as it is expected when the line of sight intercepts the accretion curtain. Also the presence of an iron K_α line ($EW \sim 100$ eV) associated with a reflection component onto the surface of the white dwarf or in the accretion flow is often detected. A typical exemple of such a complex spectrum is found in the IP 1RXS J173021.5-055933 (de Martino et al.

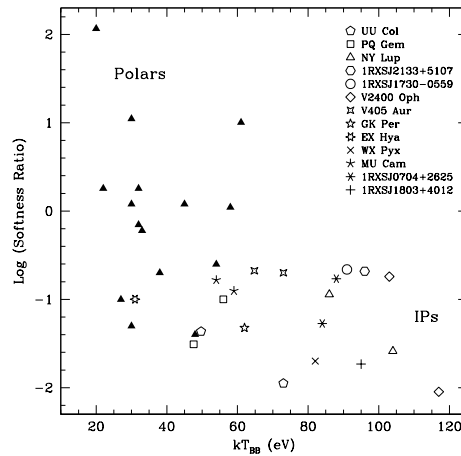


Fig. 3. Soft X-ray -to-hard X-ray ratios of magnetic CVs (from Anzolin et al. 2008). Values for polars are taken from Ramsay et al. 2004.

2008). The inclusion of these additional contributions affects the estimate of the WD masses (Hayashi et al. 2011).

4. The accretion modes in polars

Turning now to polars, among the 104 reported in Ritter & Kolb (2003) catalog, 60 have been observed so far with XMM-Newton, 9 with Chandra and 2 with Suzaku. Ramsay & Cropper (2004) and Ramsay et al. (2004) performed XMM-Newton snapshot series of 37 polars; surprisingly 16 were found to be in a low state and among the 21 in a high state, 6 do not require a soft X-ray component to fit their spectra. This fraction was confirmed with further observations analysed by Ramsay et al. (2009): among 27 polars in a high state, 10 do not exhibit any soft component.

Contrary to IPs, only 4 polars are detected at high energies with INTEGRAL, including the two asynchronous systems BY Cam and V1432 Aql (Landi et al. 2009, Scaringi et al. 2010). This is in agreement with the lower accretion rates in polars compared to IPs.

4.1. Low states and the bombardment regime

During optical low states, polars are weak X-ray emitters. Thanks to the great sensitivity of XMM-Newton a precise description of the corresponding spectra is now accessible. They are two possible X-ray emission contributors : either flux from a residual weak accretion or a coronal emission from the companion star. One of the best documented polars in low state is EF Eri which stays in this state since ten years (Schwope et al. 2007). While it is a hard X-ray source during high states, its low state spectrum is well described with an optically thin plasma at a temperature of 2.8 keV. The soft X-ray luminosity (2×10^{29} erg s⁻¹) is compatible with a coronal emission of the cool companion, but the detection of IR-optical cyclotron emission indicates that accretion is still occurring. The ratio of the cyclotron and X-ray emission of the order of 60 is in rough agreement with the bombardment solution computed by Beuermann (2004) for a magnetic field value of 14 MG and a weak specific accretion rate of 10^{-2} g cm⁻² s⁻¹. In addition X-ray flares have been detected during low states of some polars, among them VV Pup, V393 Pav (Pandel & Cordova 2002) or UZ For (Still & Mukai 2001). Coronal ejections close to the inner Lagrangian point of a 10^{17} g mass can account for the flare intensities.

The bombardment regime has also been claimed to occur in pre-polars. These sources are characterized by a high magnetic field value (derived from the position of strong cyclotron features), a very low accretion rate ($\dot{m}_{\text{dot}} < 10^{-2}$ g cm⁻² s⁻¹, a cool white dwarf ($T < 10000$ K) and an orbital period larger than 3h, except for one among 10 known objects (Schwope et al. 2009 and references herein). Only 4 are detected in X-rays as weak sources: SDSS J155331.12+551614.5 and SDSS J132411.57+032050.5 (Szkody et al. 2004), WX LMi (Vogel et al. 2007) and HS0922+1333 (Vogel et al. 2011). Their X-ray spectra are compatible with one or two optically thin plasmas (temperature of about 0.3 to 1 keV), associated with accretion in a bombardment mode from a stellar wind and with

an eventual coronal emission of a late type star companion in the saturated regime, corresponding to a constant X-ray to-bolometric luminosity ratio independent of the rotational period (Pizzolato et al. 2003). These detached systems are thought to be in a post-common envelope phase prior to a Roche lobe overflow.

4.2. Soft X-ray excess and the blobby accretion

During high states, a majority of polars exhibit a soft X-ray component which luminosity can be much higher than the hard X-ray component (ratio $L_{\text{soft}}/L_{\text{hard}} > 3$ for 5 among 21 sources (Ramsay & Cropper 2004). An extreme case is V1309 Ori with a ratio greater than 6700 (Schwarz et al. 2005). Two other examples recently described are AI Tri (Traulsen et al. 2010) and QS Tel (Traulsen et al. 2011). The corresponding X-ray light curves exhibit strong flickering. These X-ray properties are consistent with an inhomogeneous flow; dense blobs of matter sink deeply into the WD atmosphere, shock are buried, preventing the detection of a hard X-ray component. It is also noteworthy that all sources mentioned above, except one, have a magnetic field larger than 40 MG. This is fully consistent with a cyclotron dominated post-shock region. Note however that using the larger sample of Rosat observations, Ramsay & Cropper (2004) did not find a trend of energy balance ratio with the magnetic field.

4.3. Hard X-ray polars and stand-off shock

In the analysis of XMM-Newton polar observations made by Ramsay et al. (2009), ten sources among the 27 found in a high state show a hard component only (for BY Cam and CD Ind, the soft component is absent for one pole only). Their light curves do not show strong flickering. This tends to favor the standard shock model which prevails in a large number of IPs, with a dominating hard X-ray bremsstrahlung contribution and a reprocessed component shifted at lower energies (EUV).

This could be explained if these ten sources harbor lower magnetic fields implying larger accreting surfaces, but the B values of this sample is not yet well documented. Note that among the ten polars mentioned above, three are asynchronous systems (V1500 Cyg, BY Cam, CD Ind), reinforcing the analogy with IPs.

5. X-ray line diagnostics

For the brightest objects, high-resolution X-ray spectroscopy is now available using Chandra and XMM-Newton gratings. It reveals a lot of emission lines with a large range of ionisation potentials (see review by Ishida 2010), in agreement with the stratification in temperature and density of the PSR. The usual diagnostics for the temperature of the emitting zone is obtained from the He-like to H-like line ratio. The He-like triplet provides ratios sensitive to the density, however these ratios are affected by UV photo-excitation. To circumvent this difficulty, Mauche et al. (2003) have proposed the Fe XXII line ratio ($11.92\text{\AA}/11.77\text{\AA}$) which has the advantage to have a high critical density of the order of $5 \times 10^{13} \text{ cm}^{-3}$ and to be insensitive to temperature and photo-excitation. They have applied this diagnostic to Chandra observations of EX Hya and found a high PSR plasma density $n > 2 \times 10^{14} \text{ cm}^{-3}$. Using such line diagnostics, Girish et al. (2007) could map the temperature and density profiles in the post-shock region of AM Her, implying a $\sim 1 M_{\odot}$ white dwarf. This PSR structure is in agreement with the line velocity stratification derived from ions of different ionisation stages.

6. Concluding remarks

During the last decade, the new generation of X-ray observatories has given access to a better knowledge of the accretion processes in magnetic CVs. Although a few objects have been discovered in their size-limited sky surveys, their high sensitivity has permitted the confirmation of the magnetic nature of a large number of candidates found in either hard X-rays or optical surveys. This enlarged sample reveals an increased number of soft X-ray IPs and of hard X-ray polars, indicating, for both classes,

a wide range of values for the main physical parameters (magnetic field, accretion rate, spin and mass of the WD). The general X-ray spectral characteristics are roughly in agreement with the different accretion modes expected for specific ranges of these parameters.

However the confrontation of the observations to the models is often done using time-averaged spectra, preventing one from resolving fine viewing-angle effects. High temporal resolution spectra is only available for a very few sources (e.g. EX Hya and FO Aqr, Pekön & Balman 2011a, b), giving access to detailed studies of the orbitally and spin phase modulated absorption effects.

In the framework of the stand-off shock model, thermal instabilities are predicted together with quasi-periodic oscillations (QPOs) depending on the cooling flow functions (Langer et al., 1981, Chevalier & Imamura 1982). Such QPOs on a timescale of a few seconds are indeed detected in the optical flux of five polars but only upper limits have been reported so far in the X-rays (Imamura et al. 2000 and references herein). A new approach of this phenomenon is proposed, consisting in the production of a shock in laboratory and the subsequent search for oscillations (see C. Michaut in these proceedings).

On an observational point of view, the future X-ray satellites will have similar temporal and spectral resolving capabilities as in the optical, allowing, for instance, tomographic studies of the accreting regions of the white dwarf. Also, detailed atomic features will be accessible thanks to the X-ray calorimeter aboard Astro-H with a resolution of 4 eV at 6 keV, such as the dielectronic satellite lines of He and H-like iron lines which are additional accurate diagnostics of the physical parameters of the corresponding emitting regions (Ishida 2010).

7. Discussion

DAVID BUCKLEY : Is it still the case that there is a lack of deeply eclipsing confirmed IPs, compared to polars and if so, why do you think this is the case?

MARTINE MOUCHET : To my knowledge, there are no newly discovered eclipsing IPs.

This might be related to the statistics or to their weak (diffused) X-ray emission if it is partly eclipsed by the accretion disk.

Acknowledgements. M.M. acknowledges financial support by the GDR PCHE (CNRS) and D.d.M. by ASI INAF Contract N. I/009/10/0.

References

- Anzolin, G. et al. 2008, *A&A*, 489, 1243
 Anzolin, G. et al. 2009, *A&A*, 501, 1047
 Beuermann, K. 2004, IAU Colloquium 190, Eds S. Vriellmann and M. Cropper. ASPC Proceedings, 315, 187
 Bonnet-Bidaud, J.-M., de Martino, D., Mouchet, M. 2009, *ATel* 1895
 Brunschweiler, J. et al. 2009, *A&A*, 496, 121
 Canalle, J.B.G. et al. 2005, *A&A*, 440, 185
 Chevalier, R.A. & Imamura, J.N. 1982, *ApJ*, 261, 543
 Evans, P.A., Hellier, C. 2007, *ApJ*, 663, 1277
 Falize, E. et al. 2009, *Ast. Space Sci.*, 322, 71
 Fischer, A. & Beuermann, K. 2001, *A&A*, 373, 211
 Frank, J., King, A.R., Lasota, J.P. 1988, *A&A*, 193, 113
 Gänsicke, B. et al., 2004, *ApJ*, 613, L141
 Girish V., Rana, V.R., & Singh, K.P. 2007, *ApJ*, 658, 525
 Hayashi, T. et al. 2011, *astro-ph/1106.611v1*
 Hellier, C. 2007, *Proc. IAU Symp.* 243, eds J. Bouvier & I. Appenzeller, p325
 Imamura, J.N., Steiman-Cameron, T.Y., Wolff, M.T. 2000, *PASP*, 112, 18
 Imamura, J.N., Bryson, W.C., Steiman-Cameron, T.Y. 2008, *PASP*, 120, 171
 Ishida, M. 2010, *Space Sci. Rev.*, 157, 155
 Katajainen, S. et al. 2010, *ApJ*, 724, 165
 King, A.R., & Lasota, J.P. 1979, *MNRAS*, 188, 653
 Kuijpers, J., Pringle, J.E. 1982, *A&A*, 114, L4
 Lamb, D.Q., Master, A.R. 1979, *ApJ*, 234, L117
 Laming, J.M. 2004, *Phys. Rev. E*, 70, 057402
 Landi, R. et al. 2009, *A&A*, 392, 630
 Langer, S.H., Chanmugam, G., Shaviv, G. 1981, *ApJ*, 245, L23
 de Martino, D. et al. 2008, *A&A*, 481, 149
 de Martino, D. et al. 2009, *ATel* 2089
 Mauche, C.W., Liedahl, D.A., Fournier, K.B. 2003, *ApJ*, 588, L101
 Mukai, K. 2011, <http://asd.gsfc.nasa.gov/Koji.Mukai/iphome/catalog/alpha.html>
 Norton, A.J. et al. 2008, *ApJ*, 672, 524
 Pandel, D., Córdova, F.A. 2002, *MNRAS*, 336, 1049
 Pandel, D., Córdova, F.A. 2005, *ApJ*, 620, 416
 Pekön, Y. & Balman, S. 2011a, *The X-ray Universe 2011*, http://xmm.esac.esa.int/external/xmm_science/workshops/2011symposium/posters/Pekon.TopicC.pdf
 Pekön, Y. & Balman, S. 2011b, *MNRAS*, 411, 1177
 Pizzolato, N. et al. 2003, *A&A*, 397, 147
 Ramsay, G., & Cropper, M. 2004, *MNRAS*, 347, 497
 Ramsay, G. et al. 2004, *MNRAS*, 350, 1373
 Ramsay, G. et al. 2009, *MNRAS*, 395, 416
 Revnivtsev, M.G. et al. 2004, *Astronomy Letters*, 30, 772
 Revnivtsev, M.G. et al. 2009, *Nature*, 458, 1142
 Ritter, H., & Kolb, U. 2003, *A&A*, 404, 301 (update RKcat7.16, 2011)
 Saxton, C.J. et al. 2005, *MNRAS*, 360, 1091
 Saxton, C.J. et al. 2007, *MNRAS*, 379, 779
 Scaringi, S. et al. 2010, *MNRAS*, 401, 2207
 Schwarz, R. et al. 2005, *A&A*, 442, 271
 Schwöpe, A.D. et al. 2007, *A&A*, 469, 1027
 Schwöpe, A.D. et al. 2009, *A&A*, 500, 867
 Still, M. & Mukai, K. 2001, *ApJ*, 562, L71
 Suleimanov, V., Revnivtsev, M., Ritter, H. 2005, *A&A*, 435, 191
 Suleimanov, V. et al. 2008, *A&A*, 491, 525
 Szkody, P. et al. 2004, *Astron. J.*, 128, 2443
 Traulsen, I. et al. 2010, *A&A*, 516, A76
 Traulsen, I. et al. 2011, *A&A*, 529, 116
 Vogel, J., Schwöpe, A.D., & Gänsicke, B.T. 2007, *A&A*, 464, 647
 Vogel, J., Schwöpe, A.D., & Schwarz, R. 2011, *A&A*, 530, A117
 Wickramasinghe, D.T. & Ferrario L. 2000, *PASP*, 112, 873
 Woelk, U., & Beuermann, K. 1996, *A&A*, 306, 232
 Wu, K. 2000, *Space Science Rev.*, 93, 611
 Wu, K., et al. 2001, *MNRAS*, 327, 208
 Yuasa, T. et al. 2010, *A&A*, 520, A25